Chemistry International 9(3) (2023) 77-85

International Scientific Organization
http://iscientific.org/
Chemistry International
www.bosaljournals.com/chemint/

Antibacterial studies of molecularly engineered graphitic carbon nitride (g-C_3N_4) to quaternary ammonium hydroxide (g-C_3N_4-OH) composite: An application towards generating new antibiotics

Ibrahim Muhammad* and Jamilu Usman

Department of Chemistry, Faculty of Science, Sokoto State University, Along Birnin Kebbi Road, Sokoto, P.M.B. 2134, Nigeria
*Corresponding author's E. mail: ibrahimmuhammad959@gmail.com

A R T I C L E I N F O

Article type:
Research article
Article history:
Received January 2023
Accepted April 2023
July 2023 Issue
Keywords:
Functionalization
g-C_3N_4
Quaternary ammonium hydroxide
Antibacterial agent
Drug resistance

A B S T R A C T

A new molecular modification of graphitic carbon nitride (g-C_3N_4) scaffold to functionalize quaternary ammonium hydroxide (g-C_3N_4-OH) by transforming the surface $-NH_2$ and $-NH$ functional groups to quaternary methyl ammonium iodide via treatment with methyl iodide followed by exchange of ion with 0.1 M KOH is demonstrated. The g-C_3N_4-OH was characterized using XRD, FTIR, FESEM, HRTEM, and acid-base titration. Tested as an antibacterial agent for the first time, the synthesized g-C_3N_4-OH composite demonstrated an excellent inhibitory activity that range between 4 to 19 mm against standard laboratory strains of *Staphylococcus aureus* (gram +ve), *Bacillus subtilis* (gram +ve), *Escherichia coli* (gram –ve) and *Pseudomonas aeruginosa* (gram –ve). More importantly, the g-C_3N_4-OH composite is more activite on gram negative bateria.

Capsule Summary: The surface $-NH_2$ and $-NH$ functional groups of graphitic carbon nitride (g-C_3N_4) have been modified to quaternary ammonium hydroxide (g-C_3N_4-OH) composite which demonstrated an excellent antibacterial activity.

Cite This Article As: I. Muhammad and J. Usman. Antibacterial studies of molecularly engineered graphitic carbon nitride (g-C_3N_4) to quaternary ammonium hydroxide (g-C_3N_4-OH) composite: An application towards generating new antibiotics. Chemistry International 9(3) (2023) 77-85.
https://doi.org/10.5281/zenodo.8117770

INTRODUCTION

Naturally, bacteria have an ability of transferring from one to another person and also fight against the drugs that are used for the prevention of diseases (Muhammad et al., 2020; Halilu et al., 2016). Even though pharmaceutical industries have done many efforts to address this issue by producing various forms of antibiotics during the past decades, there is still an increased in resistance to these drugs by the microorganisms (Muhammad et al., 2020; Sreenivasa et al., 2012), hence the need to develop new drugs. In response to these challenges carbon nitrides belongs to a group of compounds that are polymeric in nature and can be obtained through replacement of the carbon atoms with nitrogen. Because of their abundant nitrogen, chemical and thermal stability, tunable band gaps and readily tailorable surface chemistry, carbon nitride has attracted attention greatly in the field of heterogeneous catalysis. Among different type of available carbon nitrides, graphitic carbon nitride (g-C_3N_4) has high electron-density, surface functionalities that are basic, and presence of hydrogen-bonding motifs due to plenty of N atoms and has been extensively studied in many fields like photo-catalysis and photo-electrochemical water splitting

(Lin, 2010), CO_2 reduction (Yang et al., 2015), and degradation of pollutants using sunlight and catalysts (Wang et al., 2015). Later on, it was highly studied as a support for metals to achieve hydroxylation of benzene photocatalytically, oxidation, hydrogenation, Suzuki and Sonogashira, and Knoevenagel transformations because of its good electronic and optical properties (Verma et al., 2016). Different types of functional groups such as polyethyleneimine (PEI), amines, hydrazine, boronic acid, and phenyl groups have also been tethered with g-C_3N_4 either by chemical or physical method to capture or reduce CO_2, water splitting to H_2 or even to enhance it photoluminescence and sensing properties (Cun-Zhi et al., 2016; Zang et al., 2013). Graphitic carbon nitride (g-C_3N_4) has also gotten greater interest in biomedicine due to its special elemental composition and photoelectric properties. Its carbon and nitrogen content make it to possess an outstanding biocompatibility property that is beneficial and suitable in the field. The fluorescent characteristics and its appropriate energy level (2.7 eV) make g-C_3N_4 useful in biological imaging, antibacterial materials and photodynamic therapy (PDT) (Liu et al., 2022). Recently, it has been found to have good antibacterial activity in wastewater treatment against *Klebsiella pneumonia and Escherichia coli* (Paul et al., 2020). Also nanosheets of g-C_3N_4 (N-g-C_3N_4) treated with nitrogen plasma was reported to have largely sealed defects which increases the level of electrostatic attraction between inherent pores and that of the lipid heads resulting in an excellent inhibitory activity (Cui et al., 2019).

Due to their high chemical stability, low toxicity, non-volatility and wide antimicrobial spectrum, quaternary ammonium compounds (QACs) have been widely used in several industries such as disinfectant, surface, instrument, food, textile and leather industries for many years. Because of these advantages, they are also used on historical materials to protect them against microbial growth (Katarzyna et al., 2016). Quaternary Ammonium hydroxides were also considered as safe and suitable ingredients with excellent antimicrobial effect when employed as an agent of alkalinity in injection brine solutions formulation for meat products (Cerruto-Noya et al., 2010). Recently, quaternary ammonium compounds with polymeric properties were reported to have a good antibacterial activity when incorporated into resins. Reports show that, the polymeric characteristic is responsible for the long-term antibacterial effect because it prevents leaching of the components (Imazato et al., 1992; Pashley et al., 2011). Suitable properties were also observed and reduction of demineralization process at the tooth/restoration interface in situ when added into adhesive resins (Donmez et al., 2005; Pinto et al., 2009). In addition, [2-(methacryloyloxy)ethyl]trimethylammonium chloride was reported to be effective quaternary ammonium compound which has no cytotoxic effects against human keratinocytes when used as an antibacterial agent for sealants (Collares et al., 2017; Stopiglia et al., 2012; Isadora et al., 2019). The antimicrobial effectiveness of polymer quaternary ammonium salt–capped silver nanoparticles (PQAS–AgNPs) on *Bacillus subtilis* (*B. subtilis*) was also reported (Jingyu et al., 2019). It was found that PQAS–AgNPs revealed excellent antimicrobial activity to *B. subtilis*. The report concluded that, mechanistically PQAS–AgNPs inhibit the bacteria via destruction of the bacterial cells respiratory chain, reduction of ATP synthesis, and destruction of the cell wall and cell membrane (Jingyu et al., 2019). There are three major strategies used for the preparation of quaternary ammonium hydroxides (QAOHs) (Nakayama and Fukuda, 2007; Ochoa and Trancon, 1991; Feng et al., 2008): (1) silver oxide reaction with quaternary ammonium chloride or bromide; (2) alcoholic solution exchange of ion between quaternary ammonium chloride or bromide and potassium hydroxide; (3) electrolysis of organic quaternary salts.

Herein for the first time, we showed the $-NH_2$ and NH functional group engineering of g-C_3N_4 to the corresponding quaternary ammonium hydroxide (g-C_3N_4-OH) composite and its application as an antibacterial agent. The abundant surface $-NH_2$ and –NH functionalities were initially transformed to quaternary methyl ammonium iodide via treatment with methyl iodide followed by exchange of ions with 0.1 M KOH to obtain g-C_3N_4-OH. The as-synthesized g-C_3N_4-OH was tested for antibacterial activity against standard laboratory strains of *Staphylococcus aureus* (gram +ve), *Bacillus subtilis* (gram +ve), *Escherichia coli* (gram –ve) and *Pseudomonas aeruginosa* (gram –ve) as represented in (Scheme 1).

MATERIAL AND METHODS

Melamine, methyl iodide and all solvents were obtained from LobaChemie and used as received. Mular Hilton nutrient agar and broth were used for the antibacterial analysis. Powder X-ray diffraction (XRD) was carried out using a Bruker diffractometer (D8 Advance, Davinci) with CuK_α rays (λ = 1.5418 Å). The FTIR measurements were carried out on Bruker α – Eco-ATR IR spectrometer using ZnSe crystal in the wavenumber ranging from 400 – 4000 cm^{-1}. The morphology was observed with field emission scanning electron microscope (FESEM) and high-resolution transmission electron microscope (HRTEM, JEOL JEM-2100 Plus).

Synthesis of g-C_3N_4

In a normal synthesis of g-C_3N_4, 4.0 g of melamine was taken in an empty crucible, transferred into muffle furnace and heated at 550 °C for 4 h with heating rate of 3 °C/min. The resultant pale-yellow material with yield of 2.4 g was ground to fine powder using mortar and pestle. The material was stored in a desiccator for further treatment.

Transformation of g-C_3N_4 to g-C_3N_4-I and g-C_3N_4-OH

In an ordinary reaction, 0.5 g of g-C_3N_4 was weighed and transferred into a 50 mL round bottom flask containing 5.0 mL methanol and covered with a septum to avoid vaporization of solvent and then 2.0 mL methyl iodide was

introduced into the mixture by the use of a syringe and stirred continuously at room temperature for 24 h. The material was then washed thoroughly with ethanol to remove excess methyl iodide and dried in an oven at 40 °C for 24 h to obtain g-C_3N_4-I. To transform g-C_3N_4-I to g-C_3N_4-OH, 1g of g-C_3N_4-I was reacted with 0.1 M KOH (10 mL) at room temperature for 2 h. Then distilled water was used to wash the synthesized composite and then dried at 40 °C under vacuum for overnight and stored in a desiccator for characterization.

ensure the sterility of the medium. The Gram-positive bacteria and Gram-negative bacteria ratio of dilution was 1:1000 and 1:5000, respectively, using normal saline water. The Nutrient Agar plates were flooded with 1 mL of the inoculum and the excess was removed using Pasteur pipette. Five wells (cups) of about 6 mm in diameter were cut on each Nutrient Agar plate using a sterile cork borer and the agar plugs was removed using sterile ampoule file. The composite concentration of 12.5 mg/mL, 25 mg/mL, 50 mg/mL and 100 mg/mL was prepared and 0.5 mL of each concentration was placed in the well and allowed to settle for two hours at room

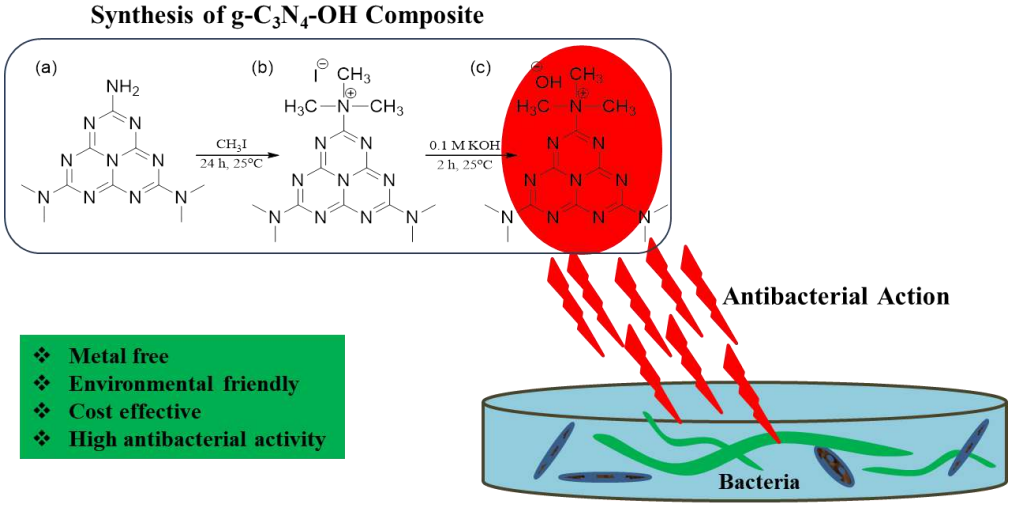

Scheme 1: Synthesis of g-C_3N_4-based quaternary ammonium hydroxide (g-C_3N_4-OH) composite and its application as an antibacterial agent.

Estimation of OH^- Concentration Produced by g-C_3N_4-OH

To estimate the OH^- concentration produced by the g-C_3N_4-OH in 20 mL of distilled water of back titration method was adopted. In a simple experiment, g-C_3N_4-OH (0.5 g) was weighed and transferred into a mixture of 20 mL distilled water containing dissolved 0.5 g NaCl, and 0.1 M HCl (10 mL) and the mixture was stirred continuously at room temperature for 24 h to ensure complete neutralization of [OH^-] released from the composite (g-C_3N_4-OH) (Fard et al., 2019). Phenolphthalein indicator 2 drops were then added to the solution and then titrated with NaOH (0.1 M) until the reaction is completed which is indicated with the appearance of pink color.

Antibacterial Tests

The antibacterial test was carried out using the well diffusion method as described by Garrod *et al.,* (1963). The Nutrient Agar plates were prepared according to manufacturer's instruction and allowed to solidify for 15 minutes at 25 °C and incubated without inoculum for 24 hours at 37 °C to temperature before incubation for 24 hours at 37 °C. Standard antibiotic The zone of inhibition was observed and was recorded using transparent ruler in millimeters (mm). Standard antibiotic Amoxicillin 12.50 mg/ml was used as reference.

Minimum Inhibitory Concentration (MIC)

This was conducted as described by Usman and Osuji (2007). The MIC was determined for the microorganisms that showed reasonable sensitivity to the test composites. The lowest concentration where no turbidity was observed was noted and considered as the Minimum Inhibitory Concentration (MIC).

Minimum Bactericidal Concentration (MBC)

The minimal bactericidal concentration was determined from broth dilution test resulting from the MIC tubes as described by Usman and Osuji (2007). The lowest concentration of the composite that showed no growth was noted and recorded as the minimum bactericidal concentration.

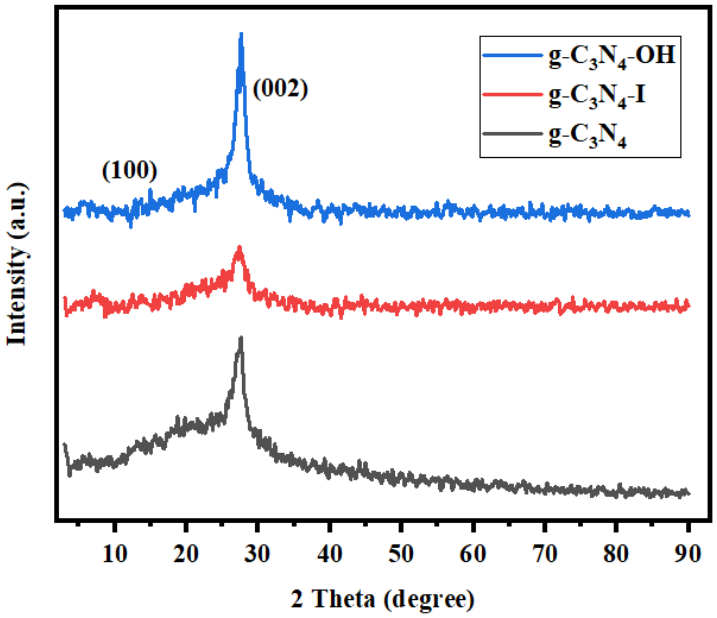

Fig. 1: Powder X-ray diffraction pattern of g-C_3N_4, g-C_3N_4-I and g-C_3N_4-OH

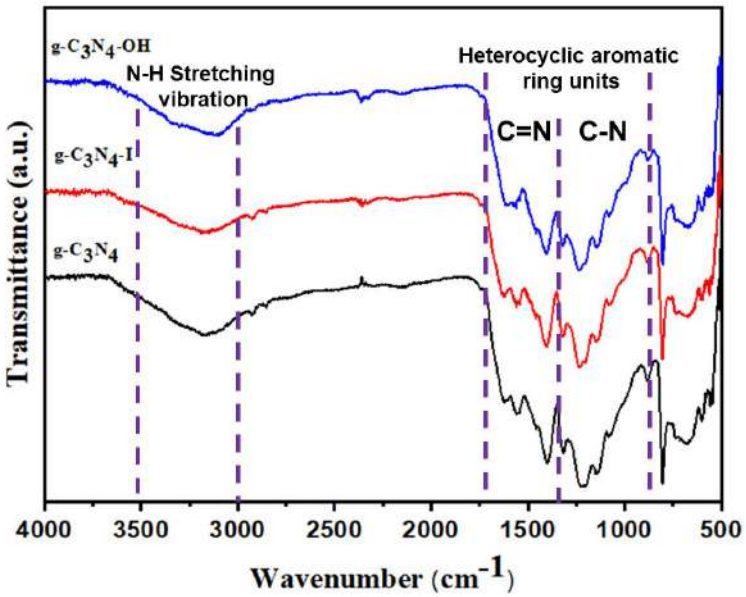

Fig. 2: FTIR spectra of g-C_3N_4, g-C_3N_4-I and g-C_3N_4-OH

RESULTS AND DISCUSSION

Characterization of materials

The crystallinity of pure g-C_3N_4, quaternary ammonium iodide (g-C_3N_4-I), and quaternary ammonium hydroxides (g-C_3N_4-OH) were determined using powder X-ray diffraction as shown in Figure 1. The pure g-C_3N_4 shows a peak of high intensity at 27.4 ° that corresponds to (*002*) reflection, which is due to the interlayer-stacking of graphite (Elavarasan et al., 2016); other peak that appears at 13.1° with very low intensity corresponds to (*100*) reflection and is assign to the motif structural packing of in-plane *tris*-s-triazine. On conversion to g-C_3N_4-I, and subsequent transformation to g-C_3N_4-OH, the features of the diffraction peaks are maintained and the intensity of (*100*) reflection is still very low. These may be as a result of possible delamination of g-C_3N_4 layer. The X-ray diffraction results indeed confirm the high stability of g-C_3N_4 toward functional group modification.

The FTIR spectra of pure and modified samples are shown in Figure 2. The broad peak absorption observed at

2900–3500 cm^{-1} is due to the presence of N-H stretching vibration (Liu et al., 2014). The peaks observed between 1000 and 1700 cm^{-1} are characteristic peaks of *tris*-s-triazine assign to C=N and C–N heterocyclic aromatic ring units as observed in the case of XRD (Yang et al., 2013). Upon conversion to g-C_3N_4-I with methyl iodide, the N-H rocking vibration intensity at 703 and 782 cm^{-1} significantly decreased, and a new band at 802 cm^{-1} appears which corresponds to OH out of plane bending vibration and these proved the g-C_3N_4-OH formation. However, functional group information of –NH and –OH stretching vibrational frequencies could not be derived in the region between 3000-3600 cm^{-1} due to overlapping.

The morphological features of the composite as further investigated with electron microscope (FESEM and HRTEM). A rod-like morphology was observed from the field emission scanning electron microscope results of pure g-C_3N_4, g-C_3N_4-I, and g-C_3N_4-OH composites (Figure 3A-C). The size of the pure g-C_3N_4 particles were found to be between 1-8 µm in length with about 150-350 nm thickness; while that of the modified g-C_3N_4-I, and g-C_3N_4-OH composite were in the range of 0.5-2.5 µm in length. The morphological features were further investigated using HRTEM, which shows rod-like particles of size approximately 0.5-2.5 µm in length as shown in Figure 3D-F. The OH^- concentration estimated by acid-base back titration was found to be 1.8 mmol/g of g-C_3N_4-OH.

Antibacterial activity of g-C_3N_4, g-C_3N_4-I and g-C_3N_4-OH

After characterization of g-C_3N_4, g-C_3N_4–I and g-C_3N_4–OH, the efficacy of the composite was investigated against standard laboratory strains of *Staphylococcus aureus* (gram +ve), *Bacillus subtilis* (gram +ve), *Escherichia coli* (gram –ve) and *Pseudomonas aeruginosa* (gram –ve). Table 1(a), 1(b), 1(c), 1(d), 1(e), 1(f) and 1(g) show the details of the results obtained from the antibacterial activity test of the pure g-C_3N_4, g-C_3N_4-I, and g-C_3N_4-OH composite. The results deduced that g-C_3N_4, g-C_3N_4-I and g-C_3N_4-OH has activity on all the bacterial strain with zone of inhibition ranging between 1.50-19.00 mm.

The pure g-C_3N_4 and g-C_3N_4-I composite a good antibacterial activity on all the test organisms at concentration of 12.5 mg/ml, 25 mg/ml, 50 mg/ml and 100 mg/ml with zone of inhibition ranging between 1.50 mm to 14 mm (Table 1a and 1b). The g-C_3N_4-OH composite exhibited excellent antibacterial activity on all the test organisms with zones of inhibition ranging between 2 mm to 19 mm (Table 1c). The pristine g-C_3N_4, g-C_3N_4-I and g-C_3N_4-OH composite showed a high level of activity on gram negative bacteria than gram positive bacteria, but all the organisms were found to be susceptible. The demonstrated activity shown by the g-C_3N_4-OH may be due to the presence of polymeric quaternary ammonium functionality that are known to have some antibacterial activity as reported by Imazato et al., 1992; Pashley et al., 2011; Jingyu et al., 2019. The results when compared with Amoxicillin (Standard Antibiotic -Table 1d), the zone of inhibition produced by the antibiotic against the test organisms was found to be appreciable in relation to those activities produced by the composite under study. However, according to Usman and Osuji (2007) diameter of zones of inhibition ≥ 10 mm are considered active. Both the pristine g-C_3N_4, g-C_3N_4-I and g-C_3N_4-OH composite were subjected

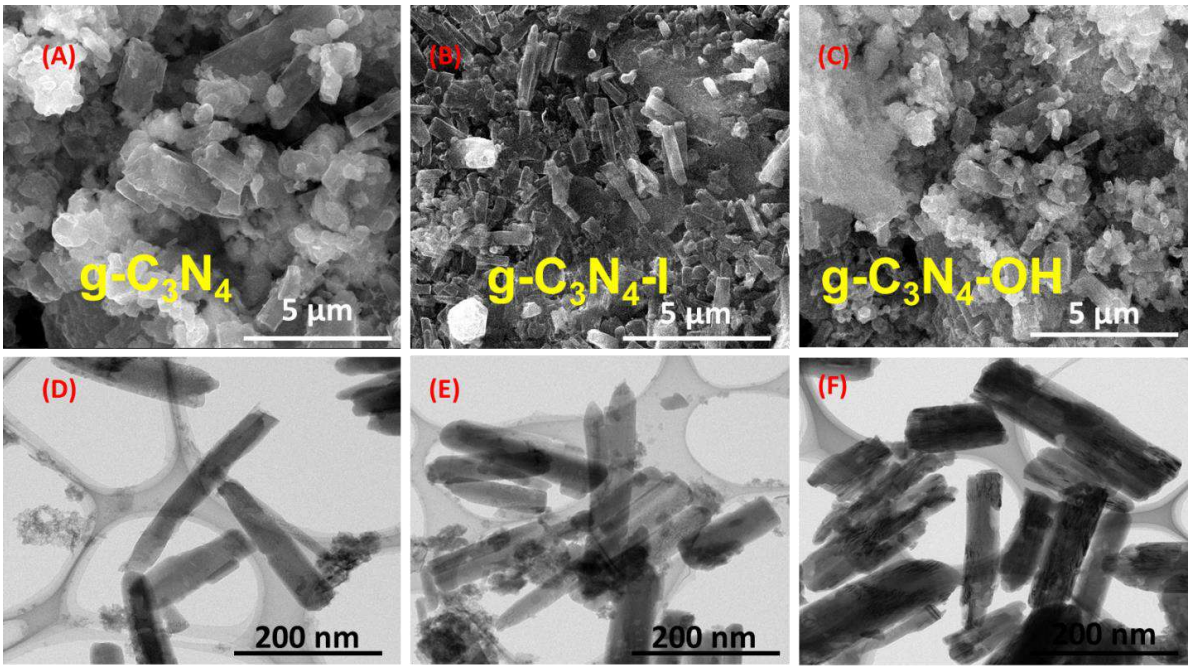

Fig. 3. FESEM images of g-C_3N_4 (A); g-C_3N_4-I (B); g-C_3N_4-OH (C); and HRTEM images of g-C_3N_4 (D); g-C_3N_4-I (E); g-C_3N_4-OH (F)

to MIC and MBC determination (Table 1e, 1f and 1g). The pristine g-C_3N_4 produced MIC of 50.0 mg/ml on *E. coli* and 25.0 mg/ml on *P.aeruginosa* while none was produce on *S. aureus* and *B. subtilis*, (Table 1e). The g-C_3N_4-I composite produced MIC of 100.0 mg/ml on *S.aureus*, 100.0 mg/ml on *B. subtillus*, 25.0 mg/ml on *E. coli* and 50.0 mg/ml on *P. aeruginosa* (Table 1f). While the g-C_3N_4-OH composite produced MIC of 100.0 mg/ml on *S.aureus*, 50.0 mg/ml on *B. subtillus*, 12.5 mg/ml on *E. coli* and 12.5 mg/ml on *P. aeruginosa* (Table 1g). The MBC results revealed that the pristine g-C_3N_4 showed no MBC on *S.aureus* and *B. subtillus*. While 50.0 mg/ml were procued on both *E. coli* and *P.*

Table 1: (a) Antibacterial activity of g-C_3N_4

Concentration (mg/ml)	Zone of Inhibition (mm)			
	S. aureus	*B. subtilis*	*E. coli*	*P. aeruginosa*
12.50	1.50	2.00	1.50	5.00
25.00	3.50	4.00	3.50	6.00
50.00	4.00	6.00	6.00	8.00
100.00	6.00	8.00	8.00	14.00

(b) Antibacterial activity of g-C_3N_4-I

Concentration (mg/ml)	Zone of Inhibition (mm)			
	S. aureus	*B. subtilis*	*E. coli*	*P. aeruginosa*
12.50	0.00	0.00	8.00	2.00
25.00	2.00	3.00	10.00	2.50
50.00	4.00	4.50	12.00	5.00
100.00	6.00	6.00	14.00	6.00

(c) Antibacterial activity of g-C_3N_4-OH

Concentration (mg/ml)	Zone of Inhibition (mm)			
	S. aureus	*B. subtilis*	*E. coli*	*P. aeruginosa*
12.50	0.00	0.00	10.00	7.00
25.00	2.00	0.00	12.00	12.00
50.00	2.00	2.50	16.00	12.00
100.00	4.00	7.00	18.00	19.00

(d) Antibacterial activity of standard antibiotic (Amoxicillin)

Antibiotic Concentration	Zone of Inhibition (mm)			
	S. aureus	*B. subtilis*	*E. coli*	*P. aeruginosa*
Amoxicillin 12.50 (mg/ml)	13.00	12.00	23.00	22.00

(e) Minimum Inhibitory Concentration (MIC) and Minimum Bactericidal Concentration (MBC) of g-C_3N_4

Test	MIC (mg/ml)	MBC (mg/ml)
S.aureus	-	-
B.subtilis	-	-
E.coli	50	50
P.aeruginosa	25	50

(f) Minimum Inhibitory Concentration (MIC) and Minimum Bactericidal Concentration (MBC) of g-C_3N_4-I

Test	MIC (mg/ml)	MBC (mg/ml)
S.aureus	100	-
B.subtilis	100	100
E.coli	25	50
P.aeruginosa	50	100

(g) Minimum Inhibitory Concentration (MIC) and Minimum Bactericidal Concentration (MBC) of g-C_3N_4-OH

Test	MIC (mg/ml)	MBC (mg/ml)
S.aureus	100	100
B.subtilis	50	100
E.coli	12.5	12.5
P.aeruginosa	12.5	12.5

aeruginosa (Table 1e). The g-C_3N_4-I showed no MBC on *S.aureus,* 100.0 mg/ml on *B. subtillus*, 50.0 mg/ml on *E. coli* and 100.0 mg/ml on *P. aeruginosa* (Table 1f). So also the g-C_3N_4-OH showed MBC of 100.0 mg/ml on *S.aureus,* 100.0 mg/ml on *B. subtillus*, 12.5 mg/ml on *E. coli* and 12.5 mg/ml on *P. aeruginosa* (Table 1g). From these results, it can be deduced that the g-C_3N_4-OH composite is bacteriostatic and bactericidal on *S.aureus* at 100.0 mg/ml, on *B. subtillus* at 50.mg/ml and 100.0 mg/ml, on *E. coli* and *P. aeruginosa at* 12.5 mg/ml.

In view of the above results, the composite showed considerable activity against *E. coli* and *P. aeruginosa*, a gram-negative bacteria known to play a significant role in many diseases (Usman and Osuji, 2007). The antibacterial activities of the composites are related to the presence of polymeric quaternary ammonium functionalities. In line with these findings, Imazato et al., 1992 and Pashley et al., 2011, reported that quaternary ammonium compounds with polymeric properties have a good antibacterial activity when incorporated into resins. The report showed that, the polymeric characteristic is responsible for the long-term antibacterial effect because it prevents leaching of the components.

In addition, [2-(methacryloyloxy)ethyl] trimethylammonium chloride was reported to be effective quaternary ammonium compound which has no cytotoxic effects against human keratinocytes when used as an antibacterial agent for resin-based sealants (Collares et al., 2017; Stopiglia et al., 2012; Isadora et al., 2019). Also the antimicrobial effectiveness of polymer quaternary ammonium salt–capped silver nanoparticles (PQAS–AgNPs) on *Bacillus subtilis* was reported. The report found that mechanistically PQAS–AgNPs inhibit the bacteria by destroying the respiratory chain of the bacterial cells, stops the synthesis of ATP, and destroyed both the cell wall and membrane (Jingyu et al., 2019).

CONCLUSION

In summary, we have demonstrated preparation of quaternary ammonium hydroxide (g-C_3N_4-OH) composite from graphitic carbon nitride (g-C_3N_4) through the molecular modification of the -NH and -NH_2 residual groups of the g-C_3N_4. The XRD data showed the composite retains its structural integrity even after the modifications with high crystallinity. The FTIR spectral data also confirmed the transformation -NH and -NH_2 functional groups and formation of g-C_3N_4-OH. The concentration of OH^- ions was found to be 1.8 mmol per gram of g-C_3N_4-OH. The g-C_3N_4-OH composite showed excellent inhibitory activity against standard laboratory strains of *Staphylococcus aureus* (gram +ve), *Bacillus subtilis* (gram +ve), *Escherichia coli* (gram –ve) and *Pseudomonas aeruginosa* (gram –ve). More importantly, the g-C_3N_4-OH composite showed more activity on gram negative bateria with zone of inhibition that range between 4-19 mm.

ACKNOWLEDGEMENT

I. Muhammad and J. Usman thanks Tertiary Education Trust Fund (Tetfund), Nigeria for their institutional base research (IBR) support (No. TETF/DR&D/CE/UNIV/SOKOTO/IBR/2022/VOL.I.) and Sokoto State University for finding this research worth doing and nominating it for the award.

REFERENCES

Adepu, A. K., Anumula, R., Narayanan, V., 2017. Photocatalytic Degradation of Rhodamine B Over a Novel Mesoporous Titanosilicate/g-C_3N_4 Nanocomposite under Direct Sunlight Irradiation. Microporous and Mesoporous Materials 247, 86–94.

Alhamami, M., Doan, H., Chil-Hung, C., 2014. A Review on Breathing Behaviors of Metal-Organic-Frameworks (MOFs) for Gas Adsorption. Materials 7, 3198-3250.

Cahn Frs, R. W., 2005. Materials Characterization, Concise Encyclopedia of Materials Characterization, Elsevier Ltd., Oxford.

Cerruto-Noya, C. A., Goad, C. L., Mireles, D. C. A., 2010. Antimicrobial Effect of Ammonium Hydroxide when Used as an Alkaline Agent in the Formulation of Injection Brine Solutions. Journal of Food Protection 74, 475–479.

Collares, F. M., Leitune, V. C. B., Franken, P., 2017. Influence of addition of [2-(methacryloyloxy)ethyl]trimethylammonium chloride to an experimental adhesive. Brazilian Oral Research 31, 28–31.

Chen, W., Chen, Z., Liu, T., Jia, Z., Liu, X., 2014. Fabrication of Highly Visible Light Sensitive Graphite-Like C_3N_4 Hybridized with $Zn_{0.28}Cd_{0.72}S$ Heterjunctions Photocatalyst for Degradation of Organic Pollutants. Journalof Environmemtal Chemical Engineering 2, 1889–1897.

Chen, Y., Lin, B., Wang, H., Yang, Y., Zhu, H., Yu, W., Basset, J. M., 2016. Surface Modification of g-C_3N_4 by Hydrazine: Simple Way for Noble-Metal Free Hydrogen Evolution Catalysts. Chemical Engineering Journal 286, 339–346.

Cui, H., Gu, Z., Chen, X., Lin, L., Wang, Z., Dai X., Yang, Z., Liu, L., Zhou, R., Dong, M., 2019. Stimulating Antibacterial Activities of Graphitic Carbon Nitride Nanosheets with Plasma Treatment. Nanoscale 11, 18416-18425.

Cun-Zhi, L., Zhen-Bo, W., Xu-Lei, S., Li-Mei, Z., Da-Ming, G., 2016. Graphitic-C_3N_4 Quantum Dots Modified Carbon Nanotubes as a Novel Support Material for a Low Pt Loading Fuel Cell Catalyst. RSC Advances 6, 32290-32297.

Donmez, N., Belli, S., Pashley, D. H., Tay, F. R., 2005. Ultrastructural correlates of in vivo/in vitro bond degradation in self-etch adhesives. *Journal of Dental Research* 84, 355–359.

Elavarasan, S., Baskar, B., Senthil, C., Bhanja, P., Bhaumik, A., Selvam, P., Sasidharan, M., 2016. An efficient mesoporous carbon nitride (g-C_3N_4) functionalized pd catalyst for

carbon–carbon bond formation reactions. RSC Advances 6, 49376–49386.

Fard, M., Ghafuri, H., Rashidizadeh, A., 2019. Sulfonated Highly Ordered Mesoporous Graphitic Carbon Nitride as a Super Active Heterogeneous Solid Acid Catalyst for Biginelli Reaction. Microporous and Mesoporous Materials 274, 83–93.

Feng, H. Z., Huang, C. H., Xu, T.W., 2008. Production of Tetramethyl Ammonium Hydroxide using Bipolar Membrane Electrodialysis. Industrial and Engineering Chemical Research 47, 7552–7557.

Garrod L. P., Waterworth, P. M., Lambert, L. D., 1963. Antibiotics and Chemotherapy, Church
Church Livingstones 4, 102-148.

Goodhew, P. J., Humphreys, J., Beanland, R., 2001. Electron Microscopy and Analysis, Taylor & Francis, London.

Goldstein, J. I., Newbury, D. E., Joy, D. C., Lyman, C. E., Echlin, P., Lifshin, E., Sawyer, L., Michael, J. R., 2003. Scanning Electron Microscopy and X-Ray Microanalysis, Kluwer Academia/Plenum Publishers, New York.

Gong, Y., Li, M., Li, H., Wang, Y., 2015. Graphitic Carbon Nitride Polymers: Promising Catalysts or Catalyst Supports for Heterogeneous Oxidation and Hydrogenation. Green Chemistry 17, 715–736.

Glusker, J. P., Lewis, M., Rossi, M., 1994. Crystal Structure Analysis for Chemists and Biologists, VCH Publishers, New York.

Habibi-Yangjeh, A., Akhundi, A., 2016. Novel Ternary *g*-C_3N_4/Fe_3O_4/Ag_2CrO_4 Nanocomposites: Magnetically Separable and Visible-light-driven Photocatalysts for Degradation of Water Pollutants. Journal of Molecular Cataysisl A-Chemical 415, 122–130.

Halilu, M. E., Muhammad, I., Dangoggo, S. M., Farouq, A. A., Ahmed, A., Shamsuddeen, A. A.,
Suleiman M., Yahaya, M., 2016. Phytochemical and antibacterial screening of petroleum ether and ethanol extracts of *Sidacordifolia* leaves. Journal of Chemical Society of Nigeria 41, 137-142.

Hattori, H., 2015. Solid base catalysts: Fundamentals and their Applications in Organic Reactions. Applied Catalysis a General abbreviation 504, 103-109.

Huang, Q., Yu, J., Cao, S., Cui, C., Cheng, B., 2015. Graphitic-C_3N_4 Quantum Dots Modified Carbon Nanotubes as a Novel Support Material for a Low Pt Loading Fuel Cell Catalyst. Applied Surface Science 358, 350–355.

Imazato, S., Kawakami, M., Torii, M., Tsuchitani, Y., 1992. Antibacterial activity of composites
containing chemically bound non-releasing antibacterial component. Journal of Dental Research 72, 721–724.

Imelik, B., Vedrine, J. C., 1994. Catalyst Characterization: Physical Techniques for Solid Materials, Plenum Press, New York.

Isadora, M. G., Stéfani, B. R., Gabriela de, S. B., Fernanda, V., Vicente, C. B. L., Fabrício, M. C., 2019. Quaternary ammonium compound as antimicrobial agent in resin-based sealants. Clinical Oral Investigation, 4-8.

Jingyu, W., Minghao, S., Zhanfang, M., Hongwei, L., Bojie, Y., 2019. Antibacterial performance of polymer quaternary ammonium salt–capped silver nanoparticles on Bacillus subtilis in water. RSC Advances 9, 25667–25676.

Katarzyna, R., Anna, K., Anna, O., Małgorzata, P., Paulina, N., Bogumił, B., Alina, K., Beata, G., 2016. Quaternary ammonium biocides as antimicrobial agents protecting historical wood and brick. Acta Biochimica Polonica 63, 153–159.

Kumar, M., Tripathi, B. P., Saxena, V. A., Shahi, K., 2009. Electrochemical Membrane Reactor: Synthesis of Quaternary Ammonium Hydroxide from its Halide by InSitu Ion Substitution. Electrochimica Acta 54, 1630-1637.

Li, Y., Jin, R., Li, G., Liu, X., Yu, M., Xing, Y., Shi, Z., 2018. Preparation of Phenyl Group Functionalized g-C_3N_4 Nanosheets with Extended Electron Delocalization for Enhanced Visible-Light Photocatalytic Activity. New Journal of Chemistry 42, 6756–6762.

Li, Y., Xu, X., Zhang, P., Gong, Y., Li, H., Wang, Y., 2013. Highly Selective Pd@mpg-C_3N_4 Catalyst for Phenol Hydrogenation in Aqueous Phase. RSC Advances 3, 10973–10982.

Lin, J., Pan, Z., Wang, X., 2014. Photochemical Reduction of CO_2 by Graphitic Carbon Nitride Polymers. ACS Sustainable Chemical Engineering 2, 353–358.

Lin, Y., 2010. Nitrogen-Doped Graphene and its Electrochemical Applications, Journal of Material. Chemistry 20, 7491-7496.

Liu, M. X., Zhang, J. Y., and Zhang, X. L. 2022. Application of graphite carbon nitride in the field of biomedicine: Latest progress and challenges, Materials Chemistry and Physics 281, 125925.

Liu, G., Tang, R., Wang, Z., 2014. Metal-free allylic oxidation with molecular oxygen catalyzed by g-C3N4 and N-Hydroxyphthalimide. Catalysis Letter 144, 717-722

Muhammad, I., Pandian, S., Hopper, W., 2020. Antibacterial and antioxidant activity of p-quinone methide derivative synthesized from 2,6-di-tert-butylphenol. Chemistry International 6, 260-266.

Nakayama, M., Fukuda, M., 2007. Electrochemical Synthesis of a Crystalline Film of Tetrabutylammonium Bromide. Solid State Ionics 178, 1095–1099.

Ochoa, G. J. R., Tarancon, E. M., 1991. Electrosynthesis of Quaternary Ammonium Hydroxides," Journal of Applied Electrochemistry 21, 365–368.

Pashley, D. H,, Tay, F. R., Imazato, S., 2011. How to increase the durability of resin-dentin bonds. Compendium Continuing Education Dental 32, 60–64.

Paul, D. R., Nehra, S. P., 2020. Graphitic carbon nitride: a sustainable photocatalyst for organic pollutant degradation and antibacterial applications. Environmental Science and Pollution Research, 1-9.

Peng, H., Mengliu, D., James, B., 2018. The Anion Effect on Zeolite Linde Type A to Sodalite PhaseTransformation. Industrial and Engineering Chemical Research 57, 10292–10302.

Pines, H., Haag, W. O., 1985. Communications - Stereoselectivity in the Carbanion-Catalyzed Isomerization of Butene. Journal of Organic Chemistry 23, 328–329.

Pinto, C. F., Leme, A. F., Ambrosano, G. M., Giannini, M., 2009. Effect of a fluoride- and bromide-containing adhesive system on enamel around composite restorations under high cariogenic challenge in situ. Journal Adhesive Dentistry 11, 293–297.

Shi, H., Chen, G., Zhang, C., Zou, Z., 2014. Polymeric g-C_3N_4 Coupled with $NaNbO_3$ Nanowires toward Enhanced Photocatalytic Reduction of CO_2 into Renewable Fuel. ACS Catalysis 4, 3637–3643.

Sreenivasa, S., Vinay, K., Mohan, N., 2012. Phytochemical analysis, antibacterial and antioxidant activity of leaf extracts of *Daturastramonium*. International Journal of Science Research 1, 83-86.

Stopiglia, C. D., Collares, F. M., Ogliari, F. A., 2012. Antimicrobial activity of [2(methacryloyloxy)ethyl] trimethylammonium chloride against Candida spp. Revista. Iberoamericana de Micologia 29, 20–23.

Streitwieser, A., Heathcock, C. H., 1989. Química Orgánica, McGraw-Hill, Mexico.

Sun, J., Fu, Y., He, G., Sun, X., Wang, X., 2015. Green Suzuki–Miyaura Coupling Reaction Catalyzed by Palladium Nanoparticles Supported on Graphitic Carbon Nitride. Applied Catalysis B Environment 165, 661–667.

Usman H., Osuji J. C., 2007. Phytochemical and In-vitro antimicrobial Assay of the Leaf Extract of *Newbouldia laevi*. African journal of traditional, Complementary andAlternative Medicines 4, 476-480.

Verma, S., Nasir Baig, R. B., Nadagouda, M. N., Varma, R. S., 2016. Selective Oxidation of Alcohols Using Photoactive VO@ g-C_3N_4. ACS Sustainable Chemical Engineering 4, 1094–1098.

Verma, S., Nasi, B. R., Nadagouda, M. N., Varma, R. S., 2017. Hydroxylation of Benzene via C–H Activation Using Bimetallic CuAg@g-C_3N_4. ACS Sustainable Chemical Engineering 5, 3637–3640.

Wang, X., Mao, W., Zhang, J., Han, Y., Quan, C., Zhang, Q., Yang, T., Yang, J., Li, X., Huang, W., 2015. Facile Fabrication of Highly Efficient g-C_3N_4/$BiFeO_3$ Nanocomposites with Enhanced Visible Light Photocatalytic Activities. Journal of Colloid and Interface Science 448, 17–23.

Wang, X. C., Maeda, K., Thomas, A., Takanabe, K., Xin, G., Carlsson, J. M., Domen, K., Antonietti, M., 2009. A Metal-Free Polymeric Photocatalyst for Hydrogen Production from Water Under Visible Light. Nature Materials 8, 76–80.

Wang, Y., and Wang, X. 2012. Polymeric Graphitic Carbon Nitride as a Heterogeneous Organocatalyst: From Photochemistry to Multipurpose Catalysis to Sustainable Chemistry. Angewandte Chemie International Edition 51, 68–89.

Wang, Y., Hai, X., Shuang, E., Chen, M., Yang, T., Wang, J., 2018. Boronic acid Functionalized g-C_3N_4 Nanosheets for Ultrasensitive and Selective Sensing of Glycoprotein in the Physiological Environment. Nanoscale 10, 4913–4920.

Xu, J., Chen, T., Shang, J. K., Long, K. Z., Li, Y. X., 2015. Facile preparation of SBA-15-Supported Carbon Nitride Materials for High-Performance Base Catalysis. Microporous and Mesoporous. Material 211, 105–112.

Yang, S. B., Gong, Y. J., Zhang, J. S., Zhan, L., Ma, L. L., Fang, Z. Y., Vajtai, R., Wang, C. X., Pulickel, M. A., 2015. Exfoliated Graphitic Carbon Nitride Nanosheets as Efficient Catalysts for Hydrogen Evolution Under Visible Light, Advance. Material 25, 2452–2456.

Yang, Y., Guo, Y., Liu, F., Yuan, X., Gao, Y., Zhang, S., Guo, W., Huo, M., 2013. Preparation and enhanced visible-light photocatalytic activity of silver deposited graphitic carbon nitride plasmonic photocatalyst. Applied Catalysis B: Environment 142-143, 828-837

Ye, C., Wang, X. Z., Li, J. X., Li, Z. J., Li, X. B., Zhang, L. P., Chen, B., Tung, C. H.,Wu, L. Z., 2016. Protonated Graphitic Carbon Nitride with Surface Attached Molecule as Hole Relay for Efficient Photocatalytic O_2 Evolution. ACS Catalalysis 6, 8336–8341.

Yu, Z., Li, F., Yang, Q., Shi, H., Chen, Q., Xu, M., 2017. Nature-Mimic Method to Fabricate Polydopamine/Graphitic Carbon Nitride for Enhancing Photocatalytic Degradation Performance. ACS Sustainable Chemical Engineering 5, 7840–7850.

Zhang, X. D., Xie, X., Wang, H., Zhang, J. J., Pan, B. C., Xie, Y., 2013. Enhanced Photoresponsive Ultrathin Graphitic-Phase C_3N_4 Nanosheets for Bioimaging. Journal of American Chemical Society 135, 18-21.

Zhang, L., Xiao, J., Wang, H., Shao, M., 2017. Carbon-Based Electrocatalysts for Hydrogen and Oxygen Evolution Reactions. ACS Catalysis. 7, 7855–7865.

Zhao, Z., Dai, Y., Lin, J., Wang, G., 2014. Highly-Ordered Mesoporous Carbon Nitride with Ultrahigh Surface Area and Pore Volume as a Superior Dehydrogenation Catalyst. Chemistryof Materials 26, 3151–3161.